Novel approach to evaluating breast density utilizing ultrasound tomography

Carri Glide,[a] Nebojsa Duric, and Peter Littrup
Karmanos Cancer Institute, 110 East Warren, Hudson-Webber Cancer Research Center, Room 7040, Detroit, Michigan 48201

(Received 29 September 2006; revised 21 November 2006;
accepted for publication 22 November 2006; published 30 January 2007)

Women with high mammographic breast density have a four- to fivefold increased risk of developing breast cancer compared to women with fatty breasts. Many preventative strategies have attempted to correlate changes in breast density with response to interventions including drugs and diet. The purpose of this work is to investigate the feasibility of assessing breast density with acoustic velocity measurements with ultrasound tomography, and to compare the results with existing measures of mammographic breast density. An anthropomorphic breast tissue phantom was first imaged with our computed ultrasound tomography clinical prototype. Strong positive correlations were observed between sound speed and material density, and sound speed and computed tomography number (Pearson correlation coefficients=0.87 and 0.91, respectively). A cohort of 48 women was then imaged. Whole breast acoustic velocity was determined by creating image stacks and evaluating the sound speed frequency distribution. The acoustic measures of breast density were evaluated by comparing these results to two mammographic density measures: (1) qualitative estimates determined by a certified radiologist using the BI-RADS Categorical Assessment based on a 1 (fatty) to 4 (dense) scale, and (2) quantitative measurements via digitization and computerized analysis of archival mammograms. A one-way analysis of variance showed that a significant difference existed between the mean values of sound speed according to BI-RADS category, while post hoc analyses using the Scheffé criterion for significance indicated that BI-RADS 4 (dense) patients had a significantly higher sound speed than BI-RADS 1, 2, and 3 at an alpha level of 0.05. Using quantitative measures of breast density, a direct correlation between the mean acoustic velocity and calculated mammographic percent breast density was demonstrated with correlation coefficients ranging from 0.75 to 0.89. The results presented here support the hypothesis that sound speed can be used as an indicator of breast tissue density. Noninvasive, nonionizing monitoring of dietary and chemoprevention interventions that affect breast density are now possible. © *2007 American Association of Physicists in Medicine*. [DOI: 10.1118/1.2428408]

Key words: breast density, ultrasound tomography, correlation, mammography

I. INTRODUCTION

Every two minutes, a woman in the United States is diagnosed with breast cancer, making it the leading cancer among American women. Identifying women who are at high risk may better enable preventive measures that have the potential to reduce the incidence of breast cancer. Mammographically dense breast tissue is strongly associated with an increased breast cancer risk, with a relative risk of up to four to five times more for the densest breast category.[1–4] In addition, mammographic density, defined as the ratio of fibroglandular to total breast areas, has been shown to be more prognostic of overall breast cancer risk than nearly all other risk factors.[5–7] Despite this compelling evidence, mammographic breast density remains a poorly recognized and not well understood risk factor for a variety of reasons.

Current breast density estimation techniques typically involve a radiologist's visual assessment of the mammograms using the four-category Breast Imaging Reporting and Data System (BI-RADS) lexicon. This subjective density classification is limited because of considerable intra- and inter-reader variability.[8,9] Furthermore, any intrinsic relationship between breast density and breast cancer risk is greatly hampered by the marked decrease in cancer detection as breast density increases.[10] Another technique employed to measure breast density involves computer-aided segmentation of digitized mammograms. This approach has proven to be more accurate, but is cumbersome and time consuming, thereby making it impractical to carry out larger studies. Finally, a mammogram is a two-dimensional (2D) projection which, by definition, does not provide an accurate volumetric estimate of the density due to the breast thickness not being taken into account. Presumably, the risk of breast cancer would have a stronger relationship to the volume of dense tissue as opposed to the projected area, which is the topic of a future paper. Despite the shortcomings of using mammography for breast density estimation, it remains the established standard of care in breast cancer screening and diagnosis, and therefore is used to evaluate the clinical relevance of our technique. To address all of these limitations, the volumetric measure that we are presenting involves a much different approach by utilizing whole-breast acoustic velocity as an overall indicator of breast density. Here, whole-breast acous-

tic velocity is defined as a global sound speed measure obtained through a sound speed histogram developed from ultrasound transmission tomograms, as described further in Sec. II.

Under assumption that tissue is fluid-like, the speed of sound (V) has the following relationship to the elastic constant (c) and material density (ρ) of the material through which it travels:

$$\mathbf{V} = \sqrt{\frac{\mathbf{c}}{\boldsymbol{\rho}}}. \quad (1)$$

From this relationship, it is apparent that the average velocity through human tissue would be related to the tissue density and elasticity. Water, which has similar properties to tissue, has a bulk elastic constant of 2.2×10^9 N/m^2.[11] In the case of myocardial tissue, there is evidence to suggest that tissue density correlates linearly with sound speed.[12] If these results extend to breast tissue, it will be possible to measure breast density quickly and safely in large trials by virtue of ultrasound's noninvasive, nonionizing nature. The feasibility of making sound speed measurements in the breast has been demonstrated historically as well as in recent scientific literature by our group, although the relationship between sound speed and breast density has yet to be investigated.[13–16]

Mammographic estimates of breast density are typically based on one mammographic view and represent a single-valued measurement. In this paper, we describe an analogous technique for obtaining a single-valued estimate of the average sound speed of the breast based on whole-breast imaging. The technique is made possible by our working clinical scanner that operates on the principles of ultrasound tomography.[16] A brief description of the scanner, a calibration of the technique with phantom measurements, and initial *in vivo* data are presented.

II. METHODS AND MATERIALS

A. CURE device

The principles of CURE, or Computerized Ultrasound Risk Evaluation, operation and image reconstruction were described previously, although a brief overview is outlined here.[16] Figure 1 (left) depicts the patient setup for the ultrasound scan, which is markedly different than that for mammography or conventional ultrasound. The patient is positioned prone with the breast situated through a hole in the canvas bedding. This results in the breast being suspended in the water tank. The water, with well-defined sound speed properties, serves as both the coupling medium and matching layer between the breast tissue and transducer. In addition, a water-coupled method permits the breast to maintain its natural shape without deformation or tissue displacement typically encountered in traditional mammographic or ultrasonic scanning. This unique imaging device produces coronal imaging similar to breast magnetic resonance, but without the pendulant effect of gravity.

The 20-cm-diam ring transducer, with an operating frequency of 1.5 MHz, encircles the breast and begins scanning near the patient's chest wall. The ultrasound signal is sequentially transmitted by each element and subsequently received with all 256 elements situated around the ring. A motorized gantry translates the ring along the breast, ranging from near the chest wall through the nipple region, as shown in Fig. 1 (right). One complete scan leads to approximately 45 tomographic slices of data per patient, taking about 1 min to image the entire breast volume. The data are then transferred to the PC workstation for reconstruction to yield sound speed images.

FIG. 1. The patient setup and clinical prototype of the CURE device. Left: Prone patient positioning for the CURE scan. Right: Close-up of the imaging tank showing the transducer ring affixed to a mechanical arm that steps the ring down while imaging the entire breast volume.

B. Phantom construction and image analysis

An anthropomorphic breast phantom, constructed by Dr. Ernest Madsen of the University of Wisconsin, provided tissue-equivalent scanning characteristics of breast tissue. Materials characteristic of fat and fibroglandular tissue contained masses ranging in size from 6 to 14 mm with varying mass densities. The phantom was scanned with the CURE device, and image reconstructions of sound speed maps were performed. For ease of image manipulation and analysis, all of the sound speed images were exported from the CURE program into the public domain software IMAGEJ, a package developed with support from the National Institute of Health (available at http://rsb.info.nih.gov/ij).[17] To preserve the sound speed measurements and units (m/s), the CURE native files were converted into ASCII images using GRID CONVERT (Geospatial Designs, Version 1.0) and subsequently imported into IMAGEJ. The images were segmented using a semiautomatic segmentation routine written in the Java language and integrated into IMAGEJ. Regions of interest (ROIs) for each phantom component were selected by applying a k-means clustering routine. This approach segments images via grouping gray-level pixels according to their proximity to randomly initialized centroid values.[18] The only user input required was to define the number of clusters used in segmentation. While it is less advantageous to introduce user input, most methods of mammographic density calculation utilize interactive thresholding that requires the user to define two different gray-level values: one associated with dense tissue and one with the image background. Statistics from the computer-defined sound speed ROIs were tabulated and correlated with the manufacturer-stated density. A correlation between the manufacturer-stated and measured CURE sound speeds is discussed in another publication.[19] In addition, a computed tomography (CT) scan taken during the construc-

TABLE I. The BI-RADS compositional category distribution for our patient population.

BI-RADS compositional category	Patient sample
1: Fatty	6
2: Scattered	23
3: Heterogeneous	15
4: Dense	4

tion of our phantom at the University of Wisconsin was analyzed using the same segmentation procedures, and a correlation was made between the sound speed and CT number for each phantom component.

C. Patient dataset

All of the patients in this study were recruited from the Walt Comprehensive Breast Center located at KCI and subsequently imaged with our in-house clinical ultrasound tomography prototype. All imaging procedures were performed under an institutional review board approved protocol and in compliance with the Health Insurance Portability and Accountability Act. The initial patient population included 48 case sets and provided a variety of breast shapes, patient ages, and breast densities.

D. Qualitative mammographic density estimates

To initially determine the feasibility of using the CURE device for breast density assessment, a sample of 48 patient mammograms was assessed according to the four BI-RADS compositional categories of: (1) almost entirely fat (<25% glandular), (2) scattered fibroglandular (25%–50% glandular), (3) heterogeneously dense (51%–75% glandular) and (4) extremely dense (>75% glandular). The American College of Radiology has established the BI-RADS categories as the current standard of care to define breast density composition.[20] Therefore, a board-certified radiologist (P.L.) with over ten years of advanced mammography experience examined the mammograms corresponding closest to the CURE exam date. Patients were assigned to a BI-RADS breast density category and their distribution is shown in Table I. The majority of the sample was distributed in the two intermediate categories, which is consistent with the findings from previous studies.[21,22] The median patient age was 48.0 years (range, 19–85).

Previous work has demonstrated substantial intra- and inter-observer variation in BI-RADS compositional category estimates.[8,9] The usage of this qualitative measure was only preliminary for our study and served to substantiate the hypothesis, thereby justifying the more involved quantitative estimation of breast density described in the next section. Further efforts were not made to evaluate the variability in the BI-RADS descriptor, particularly because this work has already been evaluated by other researchers as mentioned previously. A more rigorous method was then applied to independently estimate breast density via quantitative measurements.

E. Quantitative mammographic density measurements

Once a preliminary relationship was confirmed between acoustic velocity and BI-RADS category, a more quantitative technique was investigated to evaluate breast density. Mammograms in the craniocaudal (CC) projection were selected for 43 patients. Five patients were not included in this portion of the analysis because either they did not have mammograms available at the time of digitization, or the CURE sound speed data were corrupted in a hard drive failure. The median age for the reduced sample was 49 years (range: 28–

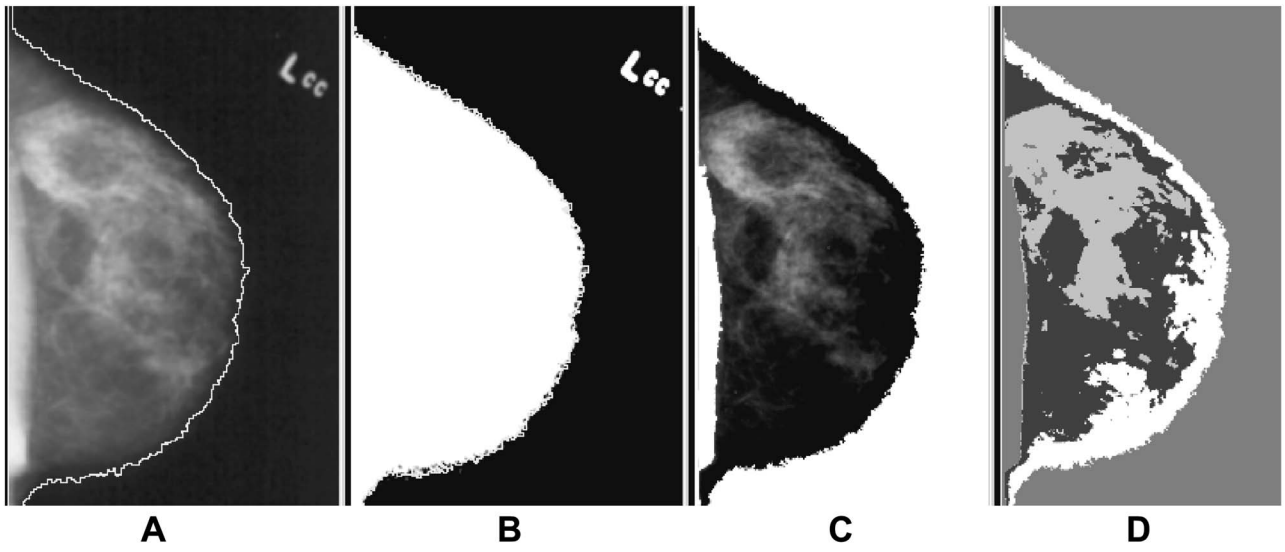

FIG. 2. (A) Craniocaudal mammogram with the breast edge defined by a mixture modeling technique, with separation between the breast area and background shown in (B). (C) Total breast area with chest wall segmented using the *k*-means cluster segmentation routine. (D) Dense area (light gray) segmented from the remaining breast area using *k*-means clustering. The mammographic percent density was calculated by dividing the dense area [light gray in (D)] by the entire breast area shown in (C).

85). The films were digitized using a Vidar VXR-16 Dosimetry Pro digitizer, a TWAIN interface (version 5.2.1), and the application of a logarithmic translation table. To ease data handling and storage, a scanning resolution of 71 dpi and 8 bit depth were utilized. Because the calculation of mammographic percent density has been shown to be a coarse measure, high resolution images were not required.[23] Previous research has shown that a representative measure of mammographic breast density can be obtained using a single CC projection of one breast due to strong left-right breast symmetry.[24] Therefore, for mammograms containing a lesion that was expected to artificially contribute to the dense area measurement, the contralateral breast CC films were used.

The goal of this study was not to develop automated software for image segmentation, but rather to evaluate the feasibility of using acoustic properties to evaluate breast density. Therefore, an interactive computer-assisted segmentation routine was implemented for two purposes: (1) to segment breast area from background and radiographic markers, and (2) to segment dense from fatty portions of the breast. To define the breast region, a mixture-modeling algorithm was employed using IMAGEJ.[17,25] This algorithm separated the gray-level histogram of an image into two classes using Gaussian modeling and calculated the image threshold as the intersection of the Gaussians as shown in Fig. 2(B). Once the background and radiographic markers were eliminated, the chest wall was segmented and deleted from the total breast area using the *k*-mean clustering technique described previously, as illustrated in Fig. 2(C). Furthermore, another iteration of the same segmentation routine was applied to the remaining breast area to segment out the dense parenchyma as shown in Fig. 2(D). Finally, the mammographic percent density was calculated as the segmented dense breast pixel area divided by the total breast pixel area (not including the chest wall) and subsequently converting this ratio into a percentage.

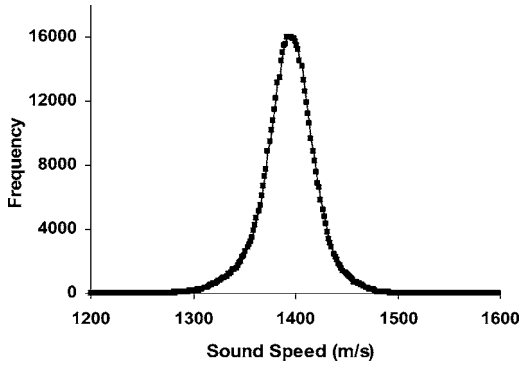

FIG. 3. Sound speed frequency distribution for a patient's breast used to determine the mean and standard deviation of volumetric sound speed.

F. Acoustic velocity (sound speed) measurements with CURE

The sound speed measurements, as described in our previous studies, are based on the signals transmitted through the breast tissue and are used to generate maps of the sound speed distribution.[16] The sound speed images are calibrated on an absolute scale in units of meters/second (m/s). Absolute calibration is possible because the arrival times of the transmitted signal are compared to water, whose sound speed is known at the time and temperature of the scan. The current spatial resolution of our transmission measurements is approximately 4 mm and measurements of sound speed can be measured to an accuracy of about ±5 m/s per voxel.[16] In addition, the thickness of each image slice is ~10 mm, generating about 45 overlapping slices for each patient so that the entire breast volume is imaged.

For ease of image manipulation and analysis, sound speed tomograms for each patient slice were exported from the CURE program into IMAGEJ. The radiologist consulted available mammograms, standard ultrasound, and CURE images

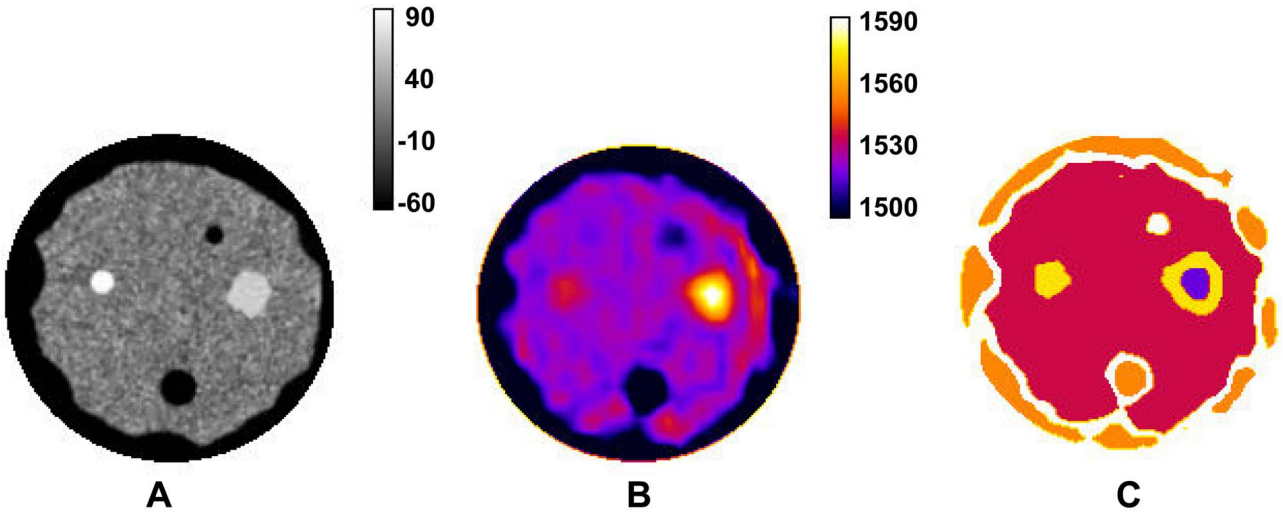

FIG. 4. (A) Shown is a CT scan of the CURE phantom. The dark areas correspond to fat inclusions and the light regions indicate dense inclusions embedded in the phantom. The scale shows the CT number of each component (unitless). (B) CURE sound speed tomogram of the CURE phantom. Note the correlation with the CT scan shown in (A). Scale demonstrates the sound speed measured in m/s. (C) *K*-means cluster segmentation (five clusters) applied to the sound speed image to distinguish regions of interest for each component's sound speed measurement.

TABLE II. The manufacturer stated density, CURE measured sound speed, and CT numbers for the segmented anthropomorphic breast phantom.

Phantom component	Density (g/cc)	Mean sound speed ±StDev (m/s)	Mean CT number ±StDev (unitless)
Large fat sphere (6:00)	0.94	1491±16	−60±6
Subcutaneous fat	0.94	1494±10	−68±27
Small fat sphere (1:00)	0.94	1510±2	−58±7
Fibroglandular tissue	1.05	1524±5	11±14
Irregular tumor (3:00)	1.07	1551±18	59±14
High attenuating tumor (9:00)	1.12	1534±3	82±6

to verify the location and extent of abnormalities (i.e., lesions) not considered part of the normal breast architecture. These abnormal lesions were segmented from the sound speed slices using the same *k*-means clustering routine described for segmenting our mammograms. Image stacks were created for each segmented patient breast, and sound speed frequency histograms were developed for entire stacks, as shown in Fig. 3. Because an image stack corresponds to the entire breast volume, the histograms represent the statistical distribution of all sound speed voxels within that breast. The histogram was then analyzed to determine the overall mean sound speed value for each breast imaged. The net result is a single-valued estimate of the average sound speed that is representative of the whole breast.

III. RESULTS

A. Phantom study

Figure 4 illustrates a CT scan, CURE sound speed tomogram, and *k*-means cluster segmentation of the sound speed tomogram for one slice of the anthropomorphic breast phantom. The fat inclusions, subcutaneous fat layer, and tumor inclusions were discernible from the surrounding fibroglandular tissue in both the CT scan and CURE sound speed tomogram. Figure 4(A) shows the CT cross section of the phantom, with the fat inclusions and subcutaneous fat layer appearing dark (low CT number) while the dense tumor-like inclusions appear light (high CT number). The *k*-means clustering routine segmented regions of interest for each phantom component and the following table summarizes the results (see Table II).

The sound speed correlation with breast density was evaluated using a Pearson correlation coefficient for two continuous variables and is shown in Fig. 5 (left). The results demonstrate a strong positive association between sound speed and material density (Pearson correlation coefficient =0.87). This same trend was observed between sound speed and CT number (Pearson correlation coefficient=0.91), also shown in Fig. 5 (right). As expected, there was a strong correlation between the CT number and mass density, with a Pearson correlation coefficient of 0.99 (not shown). To better illustrate the sound speed profile, a surface plot of the same phantom sound speed slice is shown in Fig. 6. The sound speed was elevated in the two different dense feature regions. In the velocity profile, we also observe two distinct valleys in sound speed values for the regions of fat inclusions. The difference between the large fat inclusion and surrounding fibroglandular tissue in the phantom was found to be approximately 30 m/s.

B. *In vivo* results

1. Qualitative breast density measurements

To demonstrate a relationship of our results with the current standard of care for measuring mammographic breast density, our volumetric sound speed measurements were ar-

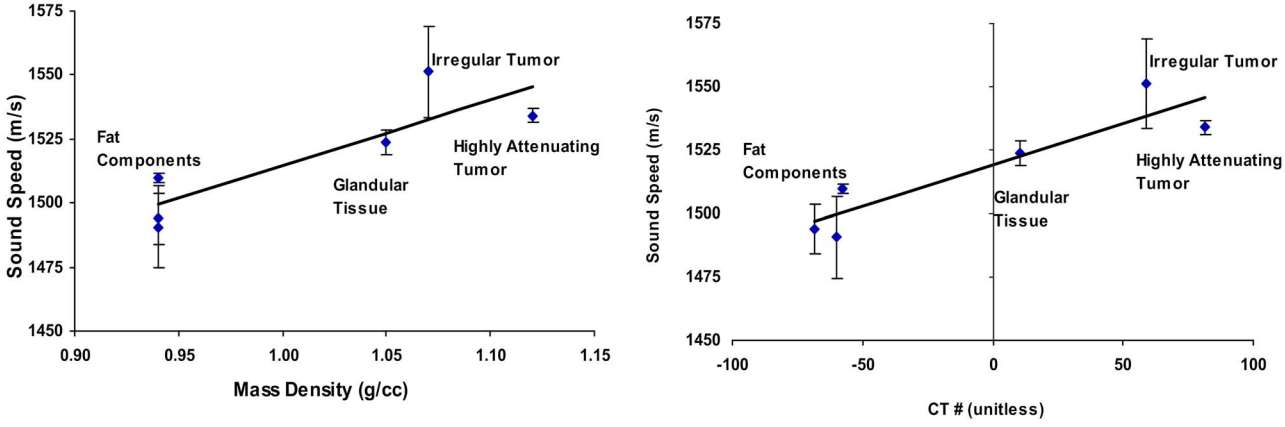

FIG. 5. A comparison of the sound speed obtained with CURE images and the mass density and CT number of each phantom component. (Left) Mass density, Pearson correlation coefficient=0.87; (right) CT number, Pearson correlation coefficient=0.91.

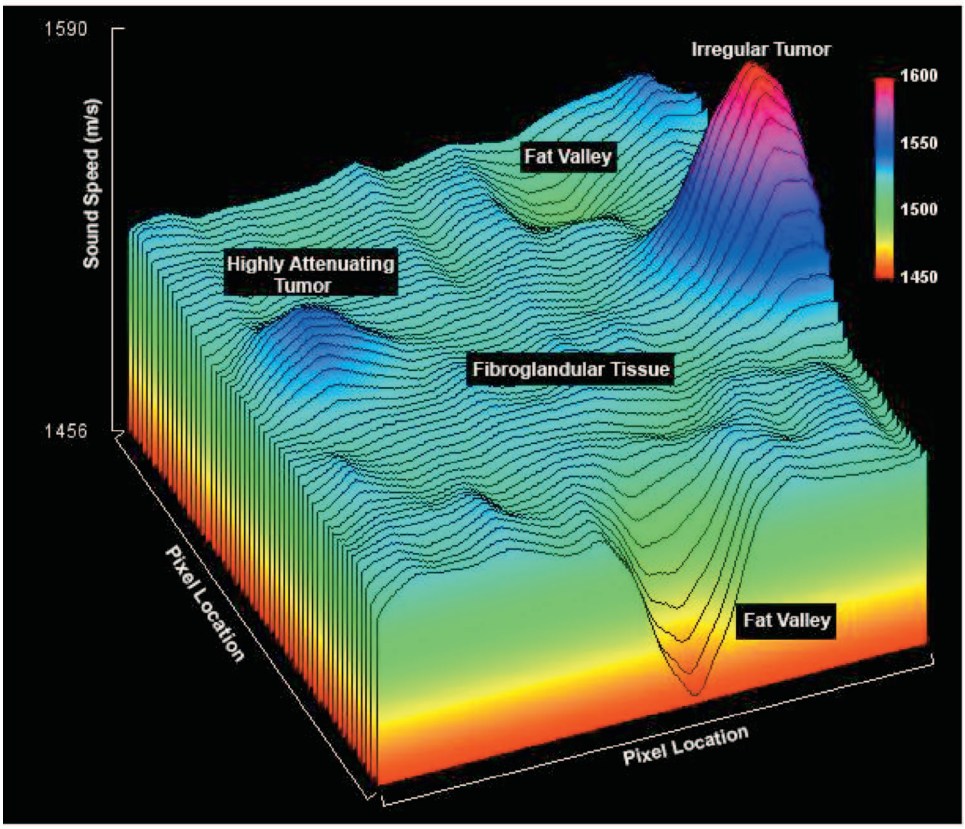

FIG. 6. The sound speed surface plot of the phantom image. The z axis is the sound speed in m/s, and the x and y directions are the pixel locations. The increased sound speeds in the regions corresponding to the tumor-like regions and the fat valleys correlating with fat inclusions are also present. The legend in the top right-hand corner indicates the sound speed in m/s.

ranged according to BI-RADS compositional category for all 48 patients. The resulting distribution is illustrated by the boxplot in Fig. 7. One extreme value, defined as more than three interquartile ranges from 25th to 75th sound speed percentiles, was detected in the BI-RADS 3 (heterogeneous) category and eliminated from the subsequent analysis. In general, an overall increase in mean sound speed was observed with increasing BI-RADS category. A one-way analysis of variance revealed that a significant difference existed between the mean values of sound speed according to BI-RADS category ($p<0.01$). Post hoc analyses using the Scheffé criterion for significance indicated that patients in the dense breast category had a significantly higher mean sound speed than patients with fatty and scattered breast densities at an alpha level of 0.05. In addition, a statistically significant difference between the mean sound speed of the

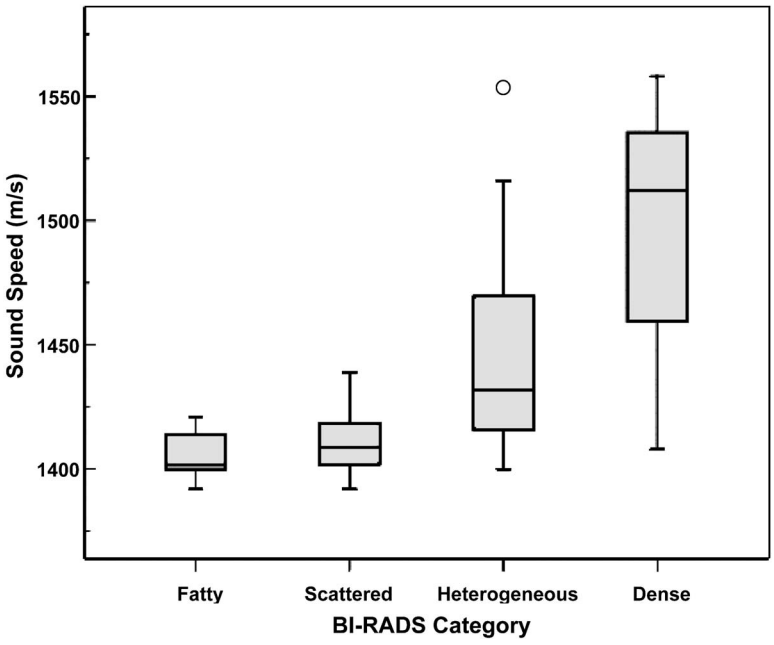

FIG. 7. Box plot of mean sound speed value for 48 patients categorized by BI-RADS compositional category. One extreme value shown was eliminated from the statistical analysis. The differences between categories (Fatty, Dense), (Scattered, Dense), and (Scattered, Heterogeneous) were all found to be significant using a one-way analysis of variance and Scheffé post hoc analysis.

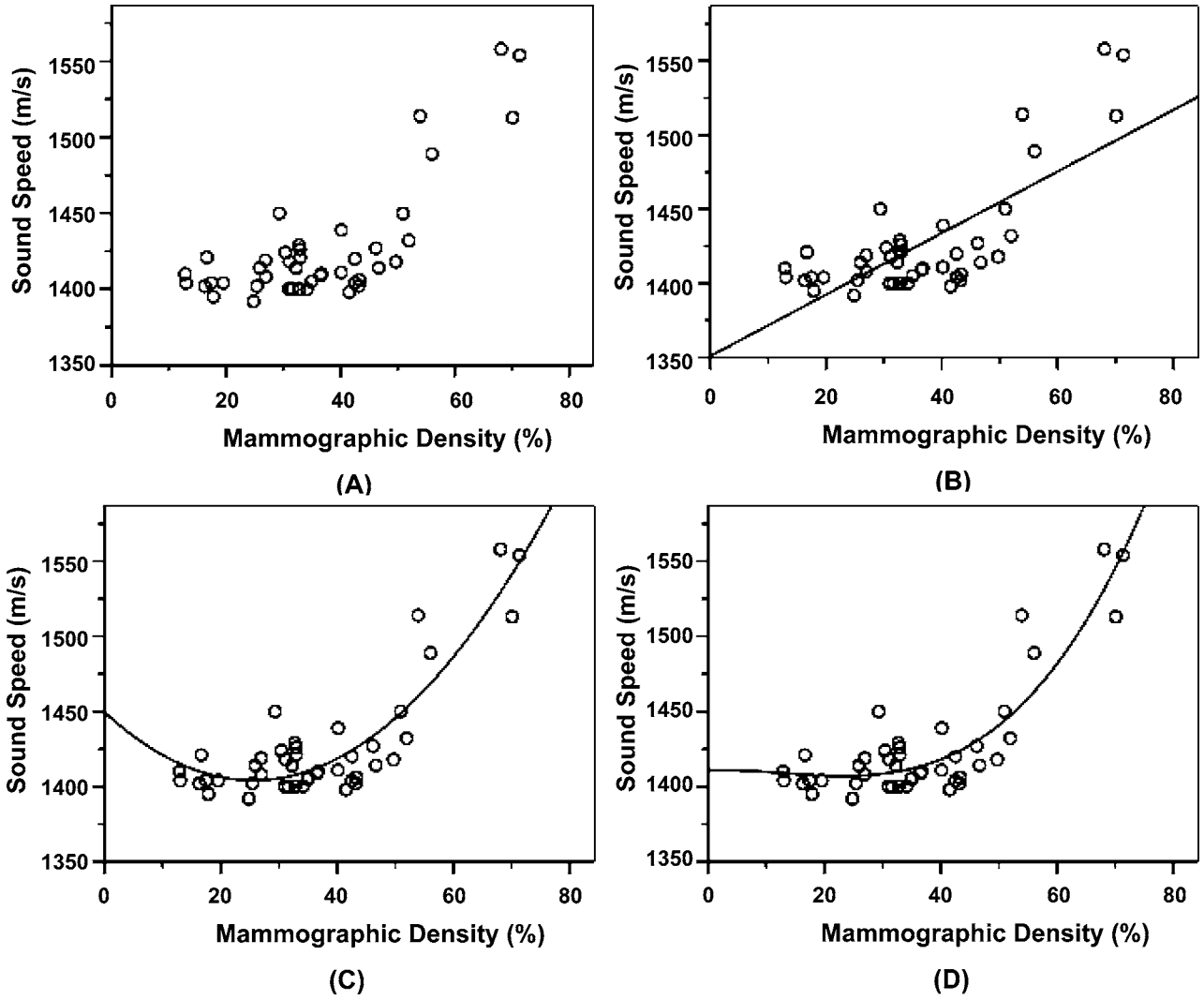

FIG. 8. A comparison of the mean sound speed measurement and quantitative percent density, obtained through digitizing and segmenting mammograms, for the reduced sample of 43 patients. (A) Observed data; (B) linear fit, correlation coefficient=0.75; (C) quadratic fit, correlation coefficient=0.89; (D) cubic fit, correlation coefficient=0.89.

scattered and heterogeneous breast patients was detected (α =0.05). The mean difference between the fatty and dense categories was approximately 92.3 m/s (standard error =21.0 m/s).

2. Quantitative breast density measurements

For the reduced sample of 43 patients, the mean mammographic percent density was 36.3±14.5% while the mean sound speed was 1426.3±39.8 m/s. Figure 8 shows the comparison between the mean sound speed and calculated mammographic percent density with corresponding curve fits. In general, sound speed increased with an increase in mammographic percent density. To better understand the empirical relationship between mammographic percent density and sound speed, least-squares fits were applied to the data and are summarized in Table III.

IV. DISCUSSION

We sought to demonstrate the feasibility of using sound speed to evaluate mass density using an anthropomorphic breast phantom. The phantom's inclusions are clearly detectable and match closely in the CT scan [Fig. 4(A)] and sound speed tomogram [Fig. 4(B)]. The reconstruction of the sound speed image is quantitative in terms of the size, location, and

TABLE III. An analysis of the relationship between mammographic percent density (x) in patient mammograms and volumetric CURE sound speed (y) obtained by least-squares fitting using different mathematical models.

Mathematical equation	Correlation coefficient	Std error of estimate
$y=1350.93+2.07x$	0.75	26.53
$y=1449.59-3.553x+0.07x^2$	0.89	18.59
$y=1410.84+0.10x-0.03x^2+0.001x^3$	0.89	18.52

sound speed of the abnormality. Furthermore, the *k*-means clustering segmentation technique applied [Fig. 4(C)] was more than adequate for differentiating each inclusion, specifically in the separation between the fatty and fibroglandular components. The irregular boundary at the fibroglandular and subcutaneous fat interface was well defined, with the former having approximately 30 m/s higher sound speed than the latter. As expected, the denser phantom materials yielded significantly higher sound speed measurements. However, the current resolution of the prototype sound speed images limits true characterization of masses below 10 mm. As a result, partial averaging of the sound speed measurements was observed between the smaller (6 mm) inclusions and adjacent fibroglandular tissue. Therefore, effects of the surrounding fibroglandular tissue reduced the sound speed for the highly attenuating tumor while increasing the sound speed for the small fat inclusion (1:00 position). Despite this limitation, this paper sought only to characterize the overall tissue content of the breasts, which was well within resolution limitations.

Figure 5 (left) shows the strong positive correlation (Pearson correlation coefficient=0.87) between sound speed and material density, which was consistent with the results previously obtained with myocardial tissue.[12] A slightly stronger correlation was observed between our measured sound speed and CT number (Pearson correlation coefficient=0.91) as shown in Fig. 5 (right). The three-dimensional surface plot shown in Fig. 6 best illustrates the magnitude of change in sound speed for different phantom components, specifically between the fibroglandular tissue and the fatty and tumor inclusions. This demonstrates the ability of using CURE sound speed tomograms to discriminate between fatty and fibroglandular tissue, a characteristic essential for the evaluation of breast density. The results presented here clearly suggest that it is feasible to utilize sound speed measurements to assess material density. These results lend support to our hypothesis, and allowed us to further this investigation *in vivo*.

Next, we obtained sound speed measurements for a sample of 48 patients. Figure 7 presents the relationship between whole-breast sound speed and qualitative breast density measures (BI-RADS categories). In general, the mean sound speed of the breast increased with increasing BI-RADS breast density category. Statistically significant differences in mean sound speed were found between the following breast density categories: (fatty, dense), (scattered, dense), and (scattered, heterogeneous). The mean difference between the fatty and dense categories was approximately 90 m/s, revealing that detectable sound speed changes according to BI-RADS category, the current standard of care, were achieved. However, the relationship between BI-RADS category and sound speed demonstrated limited clinical applicability because of the wide range of sound speed values for each breast density category. This was particularly true for BI-RADS Category 4 patients, where the standard deviation of the sound speed measurements was ~63 m/s. Wide variations in measurement can be attributed to several factors, including the coarseness of BI-RADS categories, the subjectivity involved in the radiologist's visual assessment, limited sample numbers, and the single measurement available for each patient. To further address this, we investigated the direct comparison of sound speed with calculated mammographic density, to distinguish if a continuous sound speed measurement scale may be more informative than the coarse scale currently used in the BI-RADS 4-category lexicon.

Next, we compared our sound speed measurements to mammographic percent density obtained by applying a semiautomatic segmentation routine to digitized mammograms for 43 patients. Figure 8 shows this comparison for the reduced sample size of 43 patients, and an increase in sound speed was seen with an increase in mammographic percent density. A linear fit was applied to the data points, yielding a moderate positive correlation (Pearson Correlation Coefficient=0.75). However, this linear fit was not ideal because our data exhibited an asymptotic minimum threshold representing a base line sound speed for fattier breasts. Therefore, nonlinear fitting was applied, which exhibited higher correlation coefficients (0.84, 0.89) and lower standard errors than for linear fitting. The asymptotic part of the curves shown in Fig. 8 showed that breast sound speed stayed relatively constant over the range of 0 to ~40% breast density. This result was consistent with the results demonstrated in Fig. 7 that compared sound speed to BI-RADS category. Here, the BI-RADS 1 and 2 category patients did not have a statistically significant difference, much like we observed in Fig. 8. However, breast sound speed appears to be a sensitive predictor of mammographic density in women with mammographic density greater than 40%, even with this limited patient sample. This is an important result because our methods appear to be most sensitive at the higher breast densities, where the associated breast cancer risk is also the greatest. These results indicate that the relationship between sound speed and mammographic breast density is not simple, and detailed modeling of this relationship was not warranted because of the limited number of data points used for this preliminary study.

We are continuing to recruit patients, and additional data will allow improved evaluation of the relationship between sound speed and mammographic density. In addition, we have begun the development of a model that will attempt to estimate the contribution of potential confounding factors such as breast stiffness. It is possible that breast stiffness contributes to sound speed independently of density [Eq. (1)], as may be the case for breast tissue affected by fibrocystic disease or local edema. We also attempt to model the impact of additional factors such as the effect of comparing volumetric measurements (sound speed) with area-based measurements (percent mammographic density). The results of this ongoing study will be presented in a future paper.

Some shortcomings in our current study include the coarse scale used in the BI-RADS category definition and having only one radiologist assess this parameter. However, the purpose of this study was not to reevaluate the BI-RADS descriptor, but rather to compare our sound speed measure-

ments to the current standard of care as a preliminary proof of concept. A clear advantage of using sound speed to evaluate breast density is having the potential to develop a continuous and quantitative measurement scale that would be far superior to the coarse scale of the BI-RADS categories.

Another limitation is that we imaged only 48 women for this analysis, with the majority of our sample in the intermediate breast density categories. However, this distribution is consistent with the demographic of the female population as a whole. Additional patient recruitment efforts are currently being exercised to enroll patients with dense and fatty breasts into our study. In addition, the correlation between breast density and sound speed would be better determined in a larger clinical trial that controlled for menstrual cycle in premenopausal women and allowed repeated measurements to determine intra-patient variability.

A potential shortcoming of using mammography to evaluate breast density is that the projected *area* is used, and not the entire breast volume. Tomosynthesis mammography devices are becoming available that would allow multiple sequential area estimates[26] and consideration has been given to low-dose breast CT.[27] However, ultrasound presents a distinct benefit by allowing repeated measurements without ionizing radiation concerns. Thereby, sequential measurements from dietary and/or neo-adjuvant chemotherapeutic studies cannot only measure impacts on tumor response, but also detect changes in the surrounding breast composition.

The volumetric sound speed measurement obtained in this study is representative of the entire breast, although further studies are under way to evaluate the usefulness of segmenting fibroglandular regions from the sound speed images to define an overall measurement of percent dense volume. In addition, it has been suggested that utilizing a relative measure to assess mammographic percent density may mask the extent of dense fibroglandular tissue due to the impact the total breast area has on the ratio.[28] To address this issue, a comparison can be made directly between the segmented dense mammographic area and the segmented high sound speed volume, therefore eliminating the effects of the surrounding nondense tissue. Using a volumetric measure of sound speed has the potential to more accurately define breast density than other methods currently allow, which may contribute to the understanding of the relationship between breast density and breast cancer risk.

The results presented above suggest that, from a statistical point of view, both x-ray and acoustic imaging lead to single-valued measurements that provide comparable measurements of breast density. However, our acoustic approach has potential advantages based on ultrasound's nonionizing nature in addition to the imaging device requiring minimal clinical time. A typical exam with our prototype takes approximately 5 min for patient set up and 1 min to perform the scan. Furthermore, there is no breast compression and little operator dependence. These advantages may reduce the current barriers to large-scale trials that are preventing a better understanding of the nature of the relationship between cancer risk and breast density, while providing new options for repeated monitoring of therapeutic responses and/or chemoprevention.

V. CONCLUSION

The purpose of this paper was to report on a study investigating the potential of using acoustic velocity to assess breast density. This hypothesis was evaluated using both phantom and *in vivo* data. The phantom results demonstrated that sound speed measurements are well correlated with mass density and CT number of the phantom material. Applying the same methodology of sound speed analysis to *in vivo* data yielded significant differences in the average sound speed values between the lowest and highest BI-RADS compositional categories. This result suggests that our methods of evaluating breast density are consistent with the current standard of care. Furthermore, mammograms were digitized and subsequently analyzed to evaluate the strong association that exists between breast sound speed and mammographic percent density.

While this patient sample size is limited, the preliminary results obtained in this investigation support the hypothesis that utilizing acoustical velocity, as a means to assess mammographic breast density, is feasible. By accurately identifying women who are at a higher breast cancer risk due in part to increased breast density, our approach would enable preventive measures that have the potential to monitor a quantitative variable that may correspond to eventual reduction in breast cancer incidence. Our approach to evaluating breast density has the potential to provide a safer, nonionizing, and more quantitative means of evaluating breast density, thus better elucidating the relationship that exists between breast density and breast cancer risk.

ACKNOWLEDGMENTS

The authors would like to thank Yixiang Liao and Olsi Rama for assistance in data processing and management. C.G. acknowledges the support of the Thomas C. Rumble Fellowship at Wayne State University.

[a]Author to whom correspondence should be addressed. Electronic mail: glidec@karmanos.org

[1]J. N. Wolfe, A. F. Saftlas, and M. Salane, "Mammographic parenchymal patterns and quantitative evaluation of mammographic densities: A case-control study," AJR, Am. J. Roentgenol. **148**, 1087–1092 (1987).

[2]N. F. Boyd, J. W. Byng, R. A. Jong, E. K. Fishell, L. E. Little, A. B. Miller, G. A. Lockwood, D. L. Tritchler, and M. J. Yaffe, "Quantitative classification of mammographic densities and breast cancer risk: Results from the Canadian National Breast Screening Study," J. Natl. Cancer Inst. **87**, 670–675 (1995).

[3]N. F. Boyd, G. S. Dite, J. Stone, A. Gunasekara, D. R. English, M. R. McCredie, G. G. Giles, D. Tritchler, A. Chiarelli, M. J. Yaffe, and J. L. Hopper, "Heritability of mammographic density, a risk factor for breast cancer," N. Engl. J. Med. **347**, 886–894 (2002).

[4]M. J. Yaffe, N. F. Boyd, J. W. Byng, R. A. Jong, E. Fishell, G. A. Lockwood, L. E. Little, and D. L. Tritchler, "Breast cancer risk and measured mammographic density," Eur. J. Cancer Prev. **7 Suppl 1**, 47–55 (1998).

[5]N. F. Boyd, G. A. Lockwood, J. W. Byng, D. L. Tritchler, and M. J. Yaffe, "Mammographic densities and breast cancer risk," Cancer Epidemiol. Biomarkers Prev. **7**, 1133–1144 (1998).

[6]C. Byrne, C. Schairer, J. Wolfe, N. Parekh, M. Salane, L. A. Brinton, R.

Hoover, and R. Haile, "Mammographic features and breast cancer risk: Effects with time, age, and menopause status," J. Natl. Cancer Inst. **87**, 1622–1629 (1995).
[7]J. A. Harvey and V. E. Bovbjerg, "Quantitative assessment of mammographic breast density: Relationship with breast cancer risk," Radiology **230**, 29–41 (2004).
[8]S. Ciatto, N. Houssami, A. Apruzzese, E. Bassetti, B. Brancato, F. Carozzi, S. Catarzi, M. P. Lamberini, G. Marcelli, R. Pellizzoni, B. Pesce, G. Risso, F. Russo, and A. Scorsolini, "Categorizing breast mammographic density: Intra- and interobserver reproducibility of BI-RADS density categories," Breast J. **14**, 269–275 (2005).
[9]W. A. Berg, C. Campassi, P. Langenberg, and M. J. Sexton, "Breast Imaging Reporting and Data System: inter- and intra-observer variability in feature analysis and final assessment," AJR, Am. J. Roentgenol. **174**, 1769–1777 (2000).
[10]T. M. Kolb, J. Lichy, and J. H. Newhouse, "Comparison of the performance of screening mammography, physical examination, and breast U.S. and evaluation of factors that influence them: An analysis of 27 825 patient evaluations," Radiology **225**, 165–175 (2002).
[11]R. Nave, "Bulk elastic properties," http://hyperphysics.phy-astr.gsu.edu/hbase/permot3.html.
[12]H. Masugata, K. Mizushige, S. Senda, A. Kinoshita, H. Sakamoto, S. Sakamoto, and H. Matsuo, "Relationship between myocardial tissue density measured by microgravimetry and sound speed measured by acoustic microscopy," Ultrasound Med. Biol. **25**, 1459–1463 (1999).
[13]G. Kossoff, E. K. Fry, and J. Jellins, "Average velocity of ultrasound in the human female breast," J. Acoust. Soc. Am. **53**, 1730–1736 (1973).
[14]W. Weiwad, A. Heinig, L. Goetz, H. Hartmann, D. Lampe, J. Buchmann, R. Millner, R. P. Spielmann, and S. H. Heywang-Koebrunner, "Direct measurement of sound velocity in various specimens of breast tissue," Invest. Radiol. **35**, 721–726 (2000).
[15]S. A. Goss, R. L. Johnston, and F. Dunn, "Comprehensive compilation of empirical ultrasonic properties of mammalian tissues," J. Acoust. Soc. Am. **64**, 423–457 (1978).
[16]N. Duric, P. Littrup, A. Babkin, D. Chambers, S. Azevedo, R. Pevzner, M. Tokarev, E. Holsapple, O. Rama, and R. Duncan, "Development of ultrasound tomography for breast imaging: Technical assessment," Med. Phys. **32**, 1375–1386 (2005).
[17]W. S. Rasband, "ImageJ," http://rsb.info.nih.gov/ij/.
[18]SourceForge.net, "IJ Plugins: Clustering," http://ij-plugins.sourceforge.net/plugins/clustering/index.html.
[19]N. Duric, P. Littrup, L. Poulo, A. Babkin, R. Pevzner, E. Holsapple, O. Rama, and C. Glide, "Detection of breast cancer with ultrasound tomography: First results with the computerized ultrasound risk evaluation (CURE) prototype," Med. Phys. **34**(2), 773–785 (2007).
[20]*BI-RADS Breast Imaging Reporting and Data System Breast Imaging Atlas* (American College of Radiology, Reston, VA., 2003).
[21]L. A. Venta, R. E. Hendrick, Y. T. Adler, P. DeLeon, P. M. Mengoni, A. M. Scharl, C. E. Comstock, L. Hansen, N. Kay, A. Coveler, and G. Cutter, "Rates and causes of disagreement in interpretation of full-field digital mammography and film-screen mammography in a diagnostic setting," AJR, Am. J. Roentgenol. **176**, 1241–1248 (2001).
[22]J. Brisson, C. Diorio, and B. Masse, "Wolfe's parenchymal pattern and percentage of the breast with mammographic densities: Redundant or complementary classifications?" Cancer Epidemiol. Biomarkers Prev. **12**, 728–732 (2003).
[23]J. W. Byng, N. F. Boyd, E. Fishell, R. A. Jong, and M. J. Yaffe, "Automated analysis of mammographic densities," Phys. Med. Biol. **41**, 909–923 (1996).
[24]J. W. Byng, N. F. Boyd, L. Little, G. Lockwood, E. Fishell, R. A. Jong, and M. J. Yaffe, "Symmetry of projection in the quantitative analysis of mammographic images," Eur. J. Cancer Prev. **5**, 319–327 (1996).
[25]C. Mei, M.D., "Mixture modeling," http://rsb. info.nih.gov/ij/plugins/mixture-modeling.html.
[26]H. P. Chan, J. Wei, B. Sahiner, E. A. Rafferty, T. Wu, M. A. Roubidoux, R. H. Moore, D. B. Kopans, L. M. Hadjiiski, and M. A. Helvie, "Computer-aided detection system for breast masses on digital tomosynthesis mammograms: Preliminary experience," Radiology **237**, 1075–1080 (2005).
[27]J. M. Boone and K. K. Lindfors, "Breast CT: Potential for breast cancer screening and diagnosis," Future Oncol. **2**, 351–356 (2006).
[28]G. Haars, P. A. van Noord, van C. H. van Gils, D. E. Grobbee, and P. H. Peeters, "Measurements of breast density: No ratio for a ratio," Cancer Epidemiol. Biomarkers Prev. **14**, 2634–2640 (2005).